Proceedings of the Canadian Society for Mechanical Engineering International Congress 2022
CSME Congress 2022
June 5-8, 2022, Edmonton, AB, Canada

A Semi-Empricial Correlation for Droplet Size Distribution in Swirl Nozzles

Siyu Chen[1] and Nasser Ashgriz[1]
[1]Department of Mechanical and Industrial Engineering, University of Toronto, Toronto, ON, Canada
siyuchen@mie.utoronto.ca, ashgriz@mie.utoronto.ca

Abstract— This work aims at finding a correlation for the droplet size distribution in swirl nozzles. Droplet size distributions under different operating conditions with different fluids are measured using Malvern Spraytec Dropsizer. The volume distribution can be bimodal if the volume percentage histogram given by Malvern system is unimodal. A mixture distribution with two lognormal distribution is fit to the volume distribution and exhibits good fit to both unimodal and bimodal cases. The correlations developed for the parameters gives physical interpretation of the effect of operating conditions and fluid properties on droplet sizes.

Keywords; swirl nozzle; atomization; droplet size distribution

I. INTRODUCTION

Pressure-swirl nozzles are commonly used in pharmaceutical, chemical, aerospace, and agricultural applications. They are designed to generate a swirling conical liquid sheet that eventually breaks up into ligaments and droplets. The swirling flow is usually generated by either tangentially injecting a liquid into a swirling chamber, or by having swirling structure inserted inside the nozzle (an insert). Because of having an expanding conical liquid sheet, they can generate small droplets even from large orifice diameters. Therefore, they are used in generating high mass flow industrial sprays, and also for atomizing high viscosity fluids. Their swirling behavior provides good mixing characteristics, and therefore, they are used in many chemical and propulsions system.

The droplet size distribution generated by a swirl spray nozzle not depends on the flow operating conditions and fluid properties, as well as the nozzle design. The nozzle design determines the thickness and the angle of the liquid sheet that exists the nozzle, which in turn, govern the droplet sizes that form.

A large class of correlations for the Sauter Mean Diameter (SMD or d_{32}) of a swirl spray are developed for a particular nozzle design, and they depend only on the operating conditions and fluid properties. These correlations are generally presented assuming a power law relationship, such as $SMD = C\sigma_l^a \rho_l^b \mu_l^c \dot{m}^d P^e$, where the operating conditions are presented as injecting pressure P, mass flow rate $\dot{m}$, and fluid properties as fluid density ρ_l, viscosity μ_l, and surface tension σ_l. The constant C and the exponents, a, b, c, d, e, for each term are determined by fitting to a series of experimental data.

The above correlation can also be written in terms of non-dimensional groups [1][2]. Most correlations include nondimensional groups related to operating conditions and fluid properties, such as pressure-based Reynolds number $Re_p = \sqrt{P\rho_l} d_{SC}/\mu_l$ and Ohnesorge number $Oh = \mu/\sqrt{\rho_l \sigma_l d_{or}}$, where u is velocity of the liquid sheet generated by the swirl nozzle. In addition, it can include nozzle geometry parameters, such as swirl chamber diameter, swirl chamber height, and swirl chamber inlet width. However, these correlations including geometry parameters cannot be used to predict drop size in swirl nozzle with insert. In addition, the selection of geometry parameters is different among different works. Including more factors in the correlation will give a better fit. However, it can also result in overfitting, which weaken its ability of generalizing to different testing conditions.

Another class of correlations have identified different atomization mechanisms in sprays and have attempted to improve the correlations by providing more generalized concepts. For example, Wang and Lefebvre divided the atomization process in a pressure swirl nozzle into two different stages [3]. They noted that in the first stage, the surface waves develop on the conical sheet due to instabilities. As the surface waves grow, they become large enough that some parts of the liquid break off from these surface waves and forms ligaments. The droplet size generated at this stage is related to the Reynolds number, which indicates the strength of inertial force to break up the sheet and Weber number, which governs the development of the surface wave. In the second stage, the rest of the sheet breaks up into ligaments as the surface wave grows when it moves downstream. The droplet size generated at this stage is only related to the Weber number. They presented the final SMD as a sum of the SMDs from these to process. Fitting on their experimental data resulted in the following equation. Wang and Lefebvre's model is one of the earliest models indicating that there might be multiple breakup mechanisms in the atomization process of a pressure swirl nozzle.

Most atomization models for swirl nozzles are based on instability theory for a liquid sheet. The earliest one is that

developed by Dombrowski and Johns by applying a force balance on an attenuating liquid sheet moving in the ambient gas [4]. The more commonly used one is that of Senecal et. al, referred to as the Linearized Instability Sheet Atomization (LISA) model [5]. Although, this model is developed for a non-swirling sheet, it is directly used in swirl nozzles assuming that the swirl does not change the atomization behavior. However, these atomization models usually overpredict the droplet size of the spray especially under high viscosity and high injecting pressure.

Although, SMD is a simple way of characterizing a spray, it hides the real characteristic of a spray, namely, its size distribution. The droplets in the spray have a wide range of different sizes. Predicting one characteristic droplet size for the whole spray does not give any information on the numbers of droplets with each different size. Sprays with different droplet size distributions can have similar characteristic droplet sizes. For example, a spray with some large droplets can have the same SMD as a spray with many small droplets. Therefore, the proper way to present the characteristics of a spray is to develop a correlation for the spray size distribution. SMD can then be determined directly from the size distribution. One approach to develop a droplet size distribution is known as the maximum entropy formalism (MEF). It maximizes the Shannon's entropy based on certain constraint functions such as conservation of mass, conservation of energy to find the most likely distribution functions in the spray [6][7]. Another approach is by fitting a kind of distribution function directly to the experimental results and derive a set of correlations for the parameters in the distribution function.

In this work, we are looking for a correlation for the droplet size distribution function, based on which the SMD and other statistics of spray can be determined. For this purpose, we have performed a set of experiments on a swirl nozzle and have measured the droplet size distributions for a range of operating conditions, and fluid properties. We have then developed a correlation and discuss its physical significance to the atomization process.

II. Experiment Setup

The experiments were carried out in the following testing setup. A Hydra-Cell D10 pump was used to pump fluids from the tank at pressures up to 1000 psi. The pump was controlled by both a variable frequency controller (VFD) and a pressure regulating valve to adjust the pressure at the outlet. A high accuracy pressure gauge with ±1% accuracy was used to measure the inject pressure at the nozzle inlet. Since the swirl nozzle could generate a significant number of fine droplets that either drift in the air or move with the air flow, a plastic sheet with an opening whose diameter could just let the spray pass without any blockage was mounted beneath the measuring region to reduce the number of recirculated droplets counted by the instrument.

The droplet sizes in the sprays were measured by the Malvern Spraytec Dropsizer. A 300 mm lens was used, which allowed the instrument to detect droplets from 0.1 μm to 900 μm. In order to measure the whole spray, the laser beam was aligned at the center of the conical spray. Malvern system was chosen since it provides the size distribution through a light sight, which makes it easier to develop a correlation for the size distribution. Point measurement systems, such as PDPA require a large number of measurements to obtain the size distribution across the spray. As a first attempt to determine a correlation for the size distribution, we chose Malvern system for our measurement.

In addition, an imaging system composed of a light source and a camera was used to take images of the spray to determine the position of measurement. The position of measurement was selected such that most of the liquid was atomized into droplets. Based on the images, the atomization process was completed at 8 cm from the nozzle exit for all the testing conditions. In addition, the measurements by the Malvern system at positions further than 8 cm did not show significant change in droplet sizes and distributions. As a result, the position of measurements was selected at 8 cm downward from the nozzle exit for all testing cases. Each test case was repeated for at least 3 times to check the repeatability of the experiments.

Two different swirl nozzles with inserts, named as Fine Spray Nozzles on the catalog of Spraying Systems were used in the experiment. A smaller nozzle with an orifice diameter of 0.71 mm (N1), and a larger nozzle with an orifice diameter of 1.07 mm (N2). The testing fluids used were water and water-glycerin solutions with different concentrations. The surface tension, viscosity and density were obtained through a lookup table provided by Glycerin Producers' Association [8] with linear interpolation at room temperature (20 °C) as listed in Table I. For each nozzle and each fluid, experiments were done at 3 different injection pressures of 500 psi, 700 psi, 900 psi. In order to measure the mass flow rate, the fluid was collected at the nozzle exit using a measuring cup for a certain time (more than 10 seconds) and weighted. This was repeated 3 times for each testing condition, and the average mass flow rate of the 3 runs was taken as the mass flow rate under the testing condition.

TABLE I. Fluids used and their properties

Fluid Type	Weight Percentage %	ρ_l(g/ml)	μ_l(mPa*s)	σ_l(mN/m)
Water	-	0.997	1.005	71.68
Glycerin/Water	60	1.154	10.8	67.76
	80	1.209	60.1	65.49

III. Droplet Size Distributions

The raw data given by Malvern system are in the form of histograms of volume percentages of droplets in different size bins, which are in the logarithmic scale. An example of the histograms is shown on Fig. 1. These histograms have one peak with a long tail on the left corresponding to the small droplets of less than 10 μm. Increasing the injection pressure, decreases the volume percentage of large droplets and increases those of smaller droplets. This is evident as the peaks of the curves shift to the left.

In order to study size distribution from volume percentage histograms of Fig. 1, first, they are converted to volume distributions. In the volume percentage histograms, the percentages among all size bins sums to 1, whereas in a volume

distribution, the area under the curve sums to 1 as in the probability distribution, $\int_0^\infty f(d)dd = 1$. In order to convert from volume percentage to volume distribution, the height in each bin needs to be divided by the corresponding bin width. The volume distributions for all testing cases are obtained and plotted in Fig. 2. As observed from these figures, a spray with unimodal volume histogram can have a bimodal volume distribution. The extra mode is attributed to the long tail for the small droplets in the histogram. The reason that this is not seen in the volume percentage curves is that the bin widths set in the Malvern system are not equal. Malvern is configured to increase the bin width with increasing droplet size. When a histogram with the same height in all bins is converted to the volume distribution, the bins corresponding to smaller sizes have a larger value in the distribution. This also indicates that the value for smaller droplets in volume distribution, especially those less than 10 μm (corresponding to the long tail in the histogram), are more sensitive to noise and errors in the measurement.

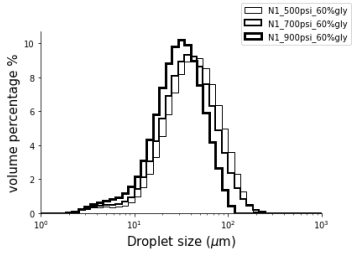

Figure 1. An example of histogram for atomizing 60% glycerine solution with Nozzle N1 at different pressure

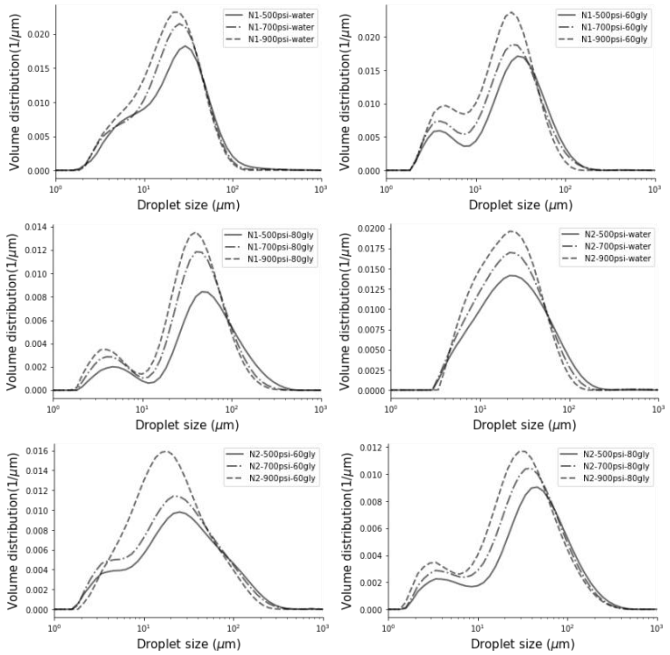

Figure 2. Volume distribution of each testing case

IV. Conversion of Volume Distribution to Size Distribution

In order to develop a generalized distribution function, and since the volume distribution for many of the cases in the present experiments are bimodal, a mixture number distribution $f_0(d)$, which is the summation of two different unimodal number distributions $f_{0,1}(d)$ and $f_{0,2}(d)$ is used to present the distribution. The following mixture number distribution is used:

$$f_0(d) = k_n f_{0,1}(d) + (1 - k_n) f_{0,2}(d).$$

The corresponding volume distribution is

$$f_3(d) = k_v f_{3,1}(d) + (1 - k_v) f_{3,2}(d),$$

where k_n is the number ratio of the droplets generated by each distribution and k_v is the volume ratio of the droplets. Since volume distribution based on a size distribution can be written as

$$f_3(d) = \frac{d^3 f_0(d)}{\int_0^\infty d^3 f_0(d) dd},$$

It can be shown that

$$k_n = \frac{k_v S_2}{S_1 + k_v(S_2 - S_1)}$$

where $S_a = \int_0^\infty d^3 f_{0,a}(d) dd$, $a = 1,2$. Therefore, as long as a bimodal distribution is fit to the volume distribution, their corresponding number distribution can be calculated.

In order to fit the data, a distribution function is needed. Instead of searching in a wide range of possible distribution functions, we are looking for some distribution function that has a physical base. One popular distribution is Gamma distribution derived from the coalescence of sub-blobs in a ligament [9]. However, we found that Gamma distribution did not work well on our data Another distribution is lognormal distribution. The lognormal distribution has the following form

$$f(d) = \frac{1}{d\sigma\sqrt{2\pi}} \exp\left(-\frac{1}{2}\left(\frac{ln(d/\mu)}{\sigma}\right)^2\right)$$

The lognormal distribution was originally developed and applied widely to describe the cascade breakup of solid particles. We first assume the number distribution of the spray is lognormal distribution. We fit the corresponding volume distribution to the experimental data. For a number distribution with lognormal distribution, the volume distribution can be found as

$$f_3(d) = \frac{d^3}{e^{3\mu+4.5\sigma^2}} f_0(d)$$

Figure 3 shows that fitting a mixture distribution with two volume distribution with lognormal distribution can also fit both bimodal and unimodal cases well. The mixture distribution has the form

$$f_3(d) = k_v f_{3,1}(d; \mu_1, \sigma_1) + (1 - k_v) f_{3,2}(d; \mu_2, \sigma_2)$$

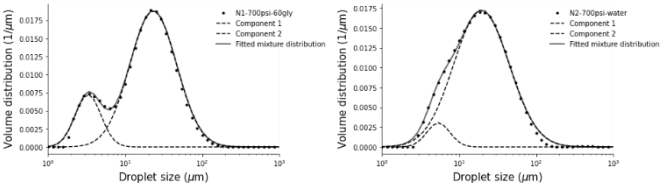

Figure 3. Fitting a mixture distribution of two volume distribution with lognormal distribution to three experiment cases.

Instead of deriving an explicit expression for number distribution for the lognormal volume distribution, Monte Carlo method is used to calculate the SMD of the fitted distribution. Since $f_3(d) \propto d^3 f_0(d)$, the fitted volume distribution function is first converted to a function proportional to number distribution by dividing d^3. Then, a sample with a large number of droplets is drawn from the function to approximate the SMD of the distribution. The number of droplets in the sample is set to 500 million such that we found the variance of the result is less than 1 μm. The SMD from the fitted distribution is listed in Table II and plotted against the measured result in Fig. 4. The fitted distribution closely matches the experimental data on the SMD, with a maximum of 6% error from the measured value.

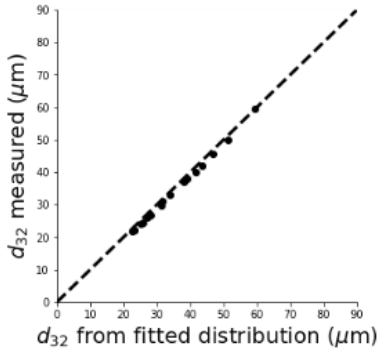

Figure 4. Comparison between SMD calculated from fitted distribution and measurement value. The dotted line is the 45-degree line.

As shown in Table II, the mode for large droplets (referred as major mode) overwhelms the mode for small droplets (referred as minor mode) in the volume distribution and takes up more than 95% of the total volume sprayed ($k_v > 0.95$) in all the testing cases. The volume ratio k_v slightly decreases as pressure increases, but it does not vary a lot. k_v also increases as the viscosity increases and mass flow rate increases (when using a nozzle with larger orifice diameter). The distances between the peak for the two modes is also large. The position of the peak for the major mode, μ_1, is larger than 30 μm, while that for the minor mode, μ_2, is always less than 7 μm. μ_1 decreases as the pressure increases and increases as the viscosity increases. σ_1 decreases as pressure increases for cases other than atomizing glycerin with nozzle N2. These properties are in accord with the trends observed from the volume distribution in Section III. However, there is no obvious trends for μ_2 and σ_2 changing with neither pressure nor viscosity. One of the reasons, as stated in Section III, is that the segment of distribution for smaller droplets is very sensitive to noise. A small change in the percentage of the sensor will largely change the shape and position of the peak. It also worth noticing that k_v is dependent on μ_2 and σ_2. The inaccuracy in the minor mode will result in a change in k_v. Since the percentage of volume taken up by the minor mode is small in all the cases and the droplet sizes for the minor mode are very small, finding a correlation for the major mode is enough in certain application to give a good correlation to predict the distribution of the spray. The SMD for using only the major mode is listed in Table II. Neglecting the minor mode will result in the prediction of SMD to be at most 20% larger than measured value. Since the amount of mass contributed by the minor mode is small and the minor mode is sensitive to noise in the current result, the distribution found in this work reduce to a lognormal volume distribution for the major mode as

$$f_3(d) = f_{3,1}(d; \mu_1, \sigma_1)$$

TABLE II. PARAMETERS IN FITTED MIXTURE DISTRIBUTION OF LOGNORMAL VOLUME DISTRIBUTIONS

Case	k_v	μ_1	σ_1	μ_2	σ_2	d_{32} (fitted)(μm)	d_{32} (major)(μm)	d_{32} (measured)(μm)	d_{32} (predicted)(μm)
1	0.955	39	0.685	6.49	0.515	27.86	33.48	27.14	40.15
2	0.975	33.63	0.675	4.8	0.425	25.75	29.09	24.55	32.54
3	0.965	30.75	0.667	5.33	0.465	23.31	26.75	21.99	27.51
4	0.98	42.25	0.675	3.85	0.38	31.19	36.51	29.67	45.77
5	0.975	37.75	0.7	3.85	0.385	27.12	32.09	26.12	38.15
6	0.955	31.38	0.623	4.69	0.475	22.74	28.09	21.86	33.3
7	0.99	83.13	0.747	4.9	0.455	59.23	67.94	59.57	62.05
8	0.988	61.13	0.658	4.38	0.42	46.81	53.37	45.57	54.18
9	0.987	54.63	0.66	3.95	0.425	41.47	47.63	40.09	48.59
10	0.99	45.88	0.897	6.3	0.38	31.51	33.16	30.97	32.31
11	0.985	38.75	0.827	6.06	0.34	28.06	29.84	26.65	26.59
12	0.97	33.75	0.752	6.91	0.35	25.31	27.61	24.19	23.09
13	0.995	69	1.055	3.22	0.32	39.01	42.14	38.04	40.46
14	0.993	58.88	1.033	3.32	0.335	33.82	37	33.19	33.43
15	0.988	75.38	0.782	4.69	0.575	51.46	60.06	49.98	55.6
16	0.988	64.75	0.808	3.96	0.505	43.71	50.49	42.09	47.85
17	0.991	57.63	0.86	3.1	0.4	38.15	42.99	37.02	42.25

V. Development of a Physical-based Correlation for Swirl Nozzle

For a lognormal distribution, μ is the mean of the log of the distribution, which determines the median of the lognormal distribution, while σ is the standard deviation of the log of the distribution, which determines the shape of the distribution. In order to relate these two parameters to parameters that have physical meanings, we referred to the LISA model.

According to LISA model, the atomization of a liquid sheet includes two steps: the breakup of liquid sheet into ligaments due to the growth of Kelvin-Helmholtz wave and the breakup of ligaments into droplets due to the growth of Rayleigh-Plateau wave. LISA model did a linear instability analysis on a liquid sheet with thickness $2a$ moving in the ambient air with a velocity u. An important parameter for the sheet breakup is the gas Weber number $We_g = \frac{\rho_g u^2 a}{\sigma_l}$. Senecal et.al pointed out that for low We_g, the growth rates of sinuous waves dominate those of the varicose waves [5]. As a result, the dispersion equation for the sinuous surface wave between the growth rate ω and wavenumber k is given by

$$\omega = -\frac{2\nu k^2 \tanh(ka)}{\rho_r + \tanh(ka)} + \frac{\left[4\nu^2 k^4 \tanh^2(ka) - \rho_r^2 u^2 k^2 - (\rho_r + \tanh(ka))\left(\rho_r u^2 k^2 + \frac{\sigma_l k^3}{\rho_l}\right)\right]^{\frac{1}{2}}}{\rho_r + \tanh(ka)}$$

where $\nu = \frac{\mu_l}{\rho_l}$ is the kinematic viscosity of the fluid, $\rho_r = \frac{\rho_g}{\rho_l}$ is the density ratio between gas medium and fluid. For $We_g > \frac{27}{16}$ (which is usually the case under high injecting pressure in industrial application), the short-wave assumption holds for the sheet breakup and $\tanh(ka) \approx 1$. If $\rho_r \ll 1$, which holds for situation such as water moving in ambient air, the dispersion equation simplifies to

$$\omega = -2\nu k^2 + (4\nu^2 k^4 + \rho_r u^2 k^2 - \frac{\sigma k^3}{\rho_l})^{\frac{1}{2}}$$

The maximum growth rate ω_{max} and its corresponding wavenumber k_{max} are found using the dispersion equation. The ω_{max} is then used to evaluate the breakup time τ and breakup length L_b as:

$$\tau = \frac{1}{\omega_{max}} \ln\left(\frac{A}{A_0}\right)$$

$$L_b = u\tau = \frac{u}{\omega_{max}} \ln\left(\frac{A}{A_0}\right)$$

where A is the amplitude of the surface wave and A_0 is the initial amplitude of the surface wave. Similarly, $\ln\left(\frac{A}{A_0}\right) = 12$. Schmidt.et al applied this to a pressure swirl nozzle and found the sheet half-thickness t_b at L_b as [10]

$$t_b = \frac{2t_{or}(d_{or} - t_{or})/cos\theta}{2L_b sin\theta + d_{or} - t_{or}}$$

According to the short-wave assumption, one ligament is formed per wavelength. The diameter of these ligaments is found using a mass balance by $d_{lig} = \sqrt{\frac{16t_b}{k_{max}}}$. As the wave grows until its amplitude reaches the ligament radius, one droplet will be generated per wavelength. The SMD of these droplets is then given using a mass balance as [11]

$$SMD = 1.882 d_{lig}(1 + 3Oh)^{\frac{1}{6}}$$

According to LISA model, the SMD of the spray is related to the characteristic diameter of ligaments, which is then determined by the dominant Kelvin-Helmholtz wavenumber k_{max}. In addition, from what observed in Section 3, the variance of the distribution is affected by the orifice diameter, which largely affect the sheet thickness. As a result, we decided to correlate μ_1 to the dominant Kelvin-Helmholtz wavelength λ_{KH} and correlate σ_1 to the sheet thickness at the orifice t_{or}.

In order to calculate these two values, the sheet velocity and the sheet thickness at the orifice needs to be determined. These two parameters can be determined from the mass flow rate, which can be directly measured in the experiment. For a swirl nozzle, the mass flow rate is $\dot{m} = (\rho u \cos\theta)\, \pi t_{or}(d_o - t_{or})$. The sheet velocity is determined using the pressure at the nozzle inlet P as $u = k_d\sqrt{2P/\rho}$, where k_d is the discharge coefficient estimated using method introduced by Tratnig and Brenn [2]. Then the sheet thickness t_{or} can be calculated from the mass flow rate.

The correlations found for the parameters are

$$\mu_1 = 1.79\lambda_{KH}^{0.604}, R^2 = 0.790$$

$$\sigma_1 = 0.072 t_{or}^{0.491}, R^2 = 0.620$$

The correlation gives a good fit for μ_1 ($R^2 = 0.790$), while that for σ_1 ($R^2 = 0.620$) is acceptable. One reason is that calculating t_{or} requires k_d, which is determined empirically. The calculated t_{or} can be different from the one in the experiment, which is hard to be measured directly. In addition, this indicates that there might be other factors involved in determining the σ_1 of the distribution.

The comparison between the SMD predicted from the distribution with parameters calculated by the correlation is calculated and listed in the Table II. Figure 5 plots these prediction against the measured SMD. For most of the cases, the SMD predicted using correlation is larger than 20% of the measurement result, which is expected because only the main peak is included in the prediction. The results that are overpredicted by more than 20% corresponds to cases atomizing water and 60% glycerin with nozzle N1. The experiment shows that these cases have a smaller k_v compared to the rest of the cases, which indicates that the minor peak may have larger effect on the overall SMD. Neglecting the small droplets in these cases may result in a larger error in the prediction.

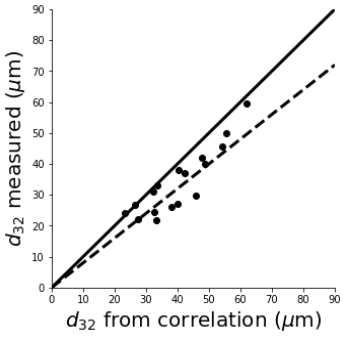

Figure 5. Comparison between SMD from the distribution with parameters calculated by the correlation and measurement value. The solid line is the 45-degree line and the dotted line stands for +20% of the measurement value.

One of the advantages of this correlation compared to a single correlation to SMD is that it reflects the effect of different parameters on the frequency of droplets with different sizes. It also reveals the effect of operating conditions and fluid properties with physical interpretations. For a lognormal distribution, the SMD will increases if μ increases or σ decreases. The correlation shows that this is equivalent to an increase in λ_{KH} or a decrease in t_{or}. These two parameters are then related to injection pressure, viscosity, orifice diameter, etc. This is very useful to explain certain phenomena. For example, as shown in Table II, atomizing 80% glycerin with nozzle N1 (smaller orifice) result in an SMD larger than that with nozzle N2 (larger orifice) under same pressure, which is different from other fluids. According to LISA model, λ_{KH} is similar under the same pressure for the two nozzles. However, the liquid sheet generated by N2 have a larger t_{or} due to the large orifice diameter, which results in a smaller SMD.

VI. Conclusion

The present work was aimed at developing a correlation for the size distribution, as opposed to the commonly reported correlation for the SMD or other average droplet sizes in the spray. Predicting a droplet size distribution gives more information on the percentage of droplets with different sizes. In addition, knowing a distribution can gives not only SMD but also other statistics.

This work used Malvern Spraytec Dropsizer to measure the sprays generated by two pressure-swirl nozzles with high injection pressure (up to 900 psi) and high viscosity fluids (up to 60 mPa.s). The histograms exhibit a peak with a long tail on the left corresponding to the droplets smaller than 10 μm. The unimodal histograms can imply a bimodal distribution where the extra mode comes from the long tail. Fitting a mixture distribution with two lognormal distributions to the volume distribution directly exhibited good fit to the experimental data with both unimodal and bimodal distribution. The d_{32} of the mixture distribution were close to the measurement result, with a maximum of 6% error. The droplets taken by the minor mode was always less than 5% of the total volume sprayed in all testing condition. Neglecting the minor mode would result in at most 20% increase in the SMD prediction.

This works gives correlations to the parameters in the lognormal distribution for the major peak as $\mu_1 = 1.79\lambda_{KH}^{0.604}$, $\sigma_1 = 0.072t_{or}^{0.491}$. The R^2 scores were 0.79 and 0.62, respectively, indicating a good fit result. The correlation for the distribution relates the SMD to parameters with physical meanings, which gives more insight on the effect of operating conditions and fluid properties on SMD.

Acknowledgements

This work was supported by International Fine Particle Research Institute (IFPRI) and NSERC.

References

[1] Richter, T., Glaser, H.W., "Auslegung von Hohlkegel-Druckdüsen," Chem.-Ing.- Tech. 59, 332–334, 1987.

[2] Tratnig, A. and Brenn, G., "Drop size spectra in sprays from pressure-swirl atomizers," International Journal of Multiphase Flow, 36(5), pp.349-363, 2010.

[3] Wang, X. F., and Lefebvre, A. H., "Atomization Performance of Pressure Swirl Nozzles," AIAA Paper, 1986.

[4] Dombrowski, N. and Johns, W., "The aerodynamic instability and disintegration of viscous liquid sheets," Chemical Engineering Science, 18(7), p.470, 1963.

[5] Senecal, P., Schmidt, D., Nouar, I., Rutland, C., Reitz, R. and Corradini, M., "Modeling high-speed viscous liquid sheet atomization. International Journal of Multiphase Flow," 25(6-7), pp.1073-1097, 1999.

[6] Li, X.; Tankin, R.S, "Droplet size distribution: a derivation of a nukiyama-tanasawa type distribution function," Comb. Sci. Technol. 56, pp. 65-76, 1987.

[7] Cousin, J., Yoon, S.J. and Dumouchel, C, "Coupling of classical linear theory and maximum entropy formalism for prediction of drop-size distribution in sprays: application to pressure swirl atomizers," Atom. Sprays, 6, pp. 601-622, 1996.

[8] Glycerin Producers'Association, "Physical properties of glycerine and its solutions," Glycerine Producers' Association, New York, 2006.

[9] Villermaux, E., Marmottant, P., Duplat, J., "Ligament-mediated spray formation," Phys. Rev. Lett. Vol. 92, Issue 7, pp. 745011-745014, 2004.

[10] Schmidt, D.P., Nouar, I., Senecal, P.K., Rutland, C.J., Martin, J.K., Reitz, R.D., "Pressure-swirl atomization in the near field," SAE Technical Paper Series 1999-01-0496, 1999.

[11] Weber, C., Zum Zerfall eines Flüssigkeitsstrahles. Z. Angew. Math. Mech. 11, 136–154, 1931.